

Design and Analyses of Electron Targets for Neutron Generation

Yousry Gohar, Henry Belch, Jose Duo, Dmitry Naberezhnev, Tanju Sofu
Argonne National Laboratory, 9700 South Cass Avenue Argonne, IL 60439, USA

Igor Bolshinsky
Idaho National Laboratory, P. O. Box 2528, Idaho Falls, ID 83403, USA

Kharkov Institute of Physics and Technology (KIPT) of Ukraine has a plan to construct a driven subcritical assembly facility using an electron accelerator. The main functions of the facility are medical isotope production and support of the Ukraine nuclear industry, including reactor physics and material research experiments. As a part of the joint activity between Argonne National Laboratory (ANL) and KIPT, ANL is developing a conceptual design for this facility. This paper describes the conceptual designs and the analyses of the electron targets generating neutrons to drive this subcritical assembly.

KEYWORD: *Electron Target Design, Tungsten Target, Uranium Target, Neutron Source, Accelerator Driven System*

1.0 Introduction

Kharkov Institute of Physics and Technology (KIPT) of Ukraine has a plan to construct an accelerator driven subcritical assembly using high enriched uranium (HEU). The main functions of the subcritical assembly are medical isotope production and support of the Ukraine nuclear industry. Reactor physics and material research experiments will be carried out utilizing this facility. The subcritical assembly is driven by an electron accelerator. The electron beam uses a target material with high atomic number for generating neutrons. The electron beam has 100-KW power and uniform spatial distribution. Argonne National Laboratory (ANL) is studying the possibility of utilizing low enrichment uranium (LEU) instead of HEU without penalizing the subcritical assembly performance. [1, 2] In addition, ANL is developing a conceptual design for the facility. This paper describes the ANL work for developing the electron target conceptual designs of the facility as part of the collaboration between ANL and KIPT.

Several studies have been carried out to investigate the target design choices and the accelerator beam parameters for a satisfactory design and an acceptable operating performance. The main focus is to maximize the neutron production from the available beam power. In addition, the target design has been configured to operate satisfactorily with electron energy in the range of 100 to 200 MeV without changing the target operating parameters. The MCNPX [3] is utilized to determine the neutron source intensity, the neutron spectrum, the spatial neutron generation, and the spatial energy deposition in the target assembly as a function of the beam parameters, the target materials, and the target design details. The Computational Fluid Dynamics (CFD) software package STAR-CD [4] is used for the thermal-hydraulics analyses. The coolant velocity profiles and the spatial temperature distributions in the target assembly have been studied using the spatial energy deposition distributions obtained from the MCNPX analyses. The NASTRAN [5] structure analysis computer code has been used to calculate the thermal stresses in the target materials using the spatial

temperature distributions from the CFD analyses. These analyses have been iterated to satisfy the temperature and the thermal stress limits for a satisfactory operation. Conceptual target designs have been developed based on the results of these studies and the engineering practices including heat transfer, thermal hydraulics, structure, fabrication, and material requirements. The target geometrical configuration has been designed to maximize the neutron source strength and the neutron utilization and to provide irradiation channels at the highest flux level. The paper presents the key results from these analyses and the electron target conceptual designs.

2.0 Physics Analyses

The electron beam generates x-rays with a continuous energy spectrum (Bremsstrahlung radiation) from the interactions with the target material. These x-rays are absorbed in a variety of photonuclear reactions in the target materials and neutrons are produced from these reactions. Target materials with high atomic number are required to enhance the neutron production. In addition, high melting point, high thermal conductivity, chemical inertness, high radiation damage resistance, and low neutron absorption cross section are the desirable properties for the target materials. The physics analyses of the possible target materials show that uranium, tungsten, lead, and tantalum produce the highest number of neutrons per electron. Figure 1 shows the calculated neutron yields from these target materials as a function of the electron energy. The physical properties of the uranium and tungsten materials, their neutron yields, and the operating experience from different accelerator facilities around the world lead to the selection of these two materials for generating neutrons. Tungsten has the highest melting point of all metals (~3695 K). Although it oxidizes in air but it has excellent corrosion resistance. Uranium target material produces the highest neutron yield per electron due to its photo-neutron production cross section and the additional neutrons from the photo- and the neutron-fission reactions. The operating lifetime of the uranium target is shorter than the tungsten target lifetime because of the extra swelling caused by fission gasses.

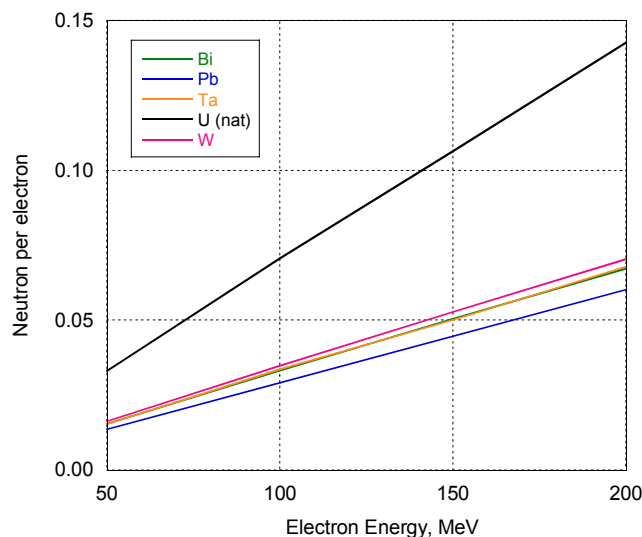


Figure 1. Neutron Yield per Electron as a Function of the Electron Energy from Different Materials

In order to characterize each target material, several performance parameters were analyzed. These parameters include but are not limited to the total neutron yield, total energy deposition,

neutron spectrum, neutron and energy deposition spatial distributions, and required target length. Each of these parameters has a particular role for defining the target performance and design. A high neutron yield enhances the neutron source intensity, which defines the neutron flux level and the total power of the subcritical assembly. The target energy deposition influences the design of the target coolant system and the neutron yield. The neutron spectrum affects the system's effectiveness for performing material characterizations and producing medical isotopes. The spatial neutron distribution of the target determines the target position inside the sub-critical assembly and the neutron source utilization. All these parameters are studied to define the target performance characteristics and the design configuration.

The performance of the tungsten and the uranium targets has been analyzed as a function of the target length for a 100 KW beam power with different electron energies. The spatial energy deposition per incident electron in the uranium target is shown in Figure 2. The peak value occurs a few millimeters away from the electron beam window. The peak increases and shifts further from the electron beam window as the electron energy increases. The spatial energy deposition normalized to 2-KW/cm² power density on the beam window is plotted in Figure 3 for different electron energies. These results show that low energy electrons deposit their energy very close to the beam window. In this case, the heat removal of the deposited energy requires the use of thin layers of the target material to avoid generating high temperature and thermal stress. The use of thin target disks results in a large number of coolant channels, which reduces the target performance. The water coolant slows down and absorbs electrons without generating neutrons. This suggests the use of a low beam power density or electron energy above 100 MeV. Reducing the beam power density increases the target cross section area and the neutron leakage from the beam tube, which reduces the neutron flux in the subcritical assembly. The use of electron energy above 100 MeV spreads the energy deposition along the beam direction and reduces the number of coolant channels. Similar conclusions are obtained for the tungsten target.

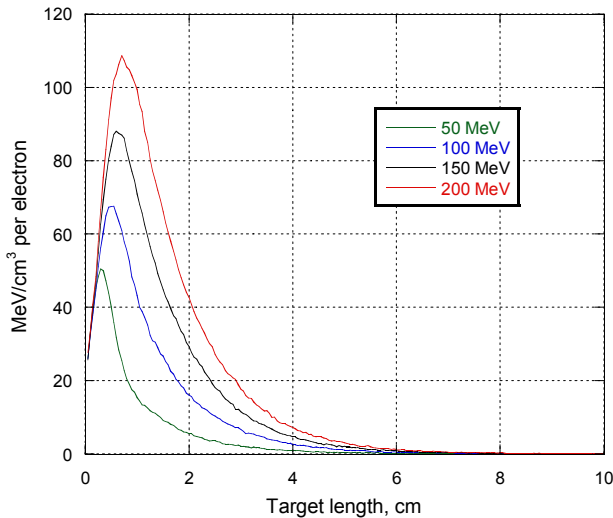


Figure 2. Spatial Energy Deposition per Electron in the Uranium Target for Different Electron Energies

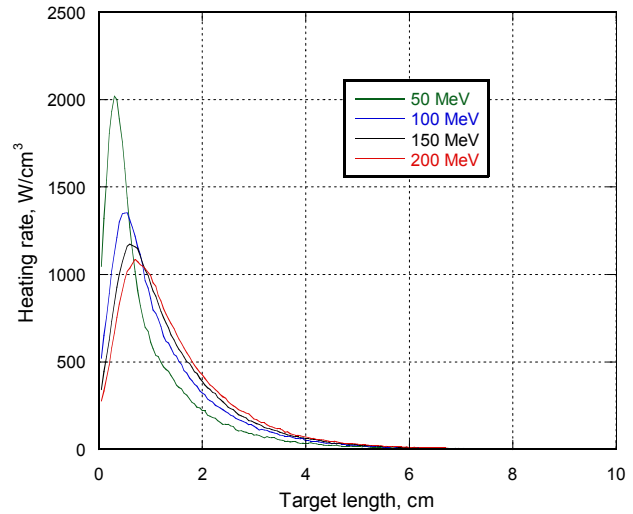


Figure 3. Spatial Energy Deposition in the Uranium Target for Different Electron Energies Normalized to 2 KW/cm² Beam Window Power Density

The neutron yield per electron is shown in Figure 4. It increases as the electron energy increases. On the other hand, the neutron source strength per second from the 100 KW beam reaches a saturation value as the electron beam energy increases above 100 MeV as shown in Figure 5. Therefore, electrons with energy above 100 MeV produce the maximum neutron source strength for the 100-KW electron beam power under consideration.

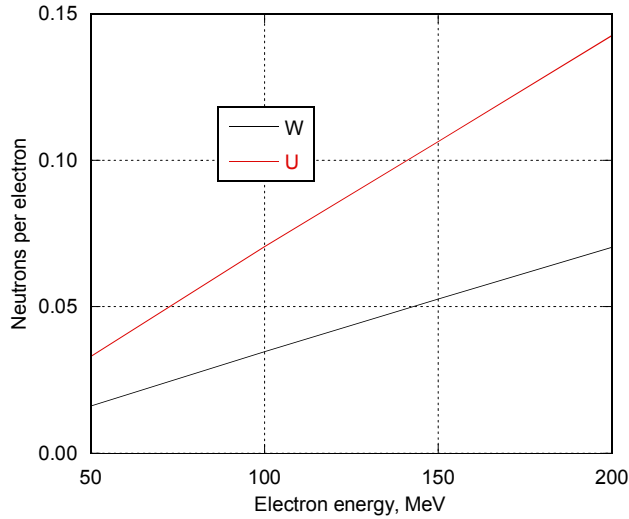


Figure 4. Neutron Yield per Electron from the Uranium and the Tungsten Targets as a Function of the Electron Energy

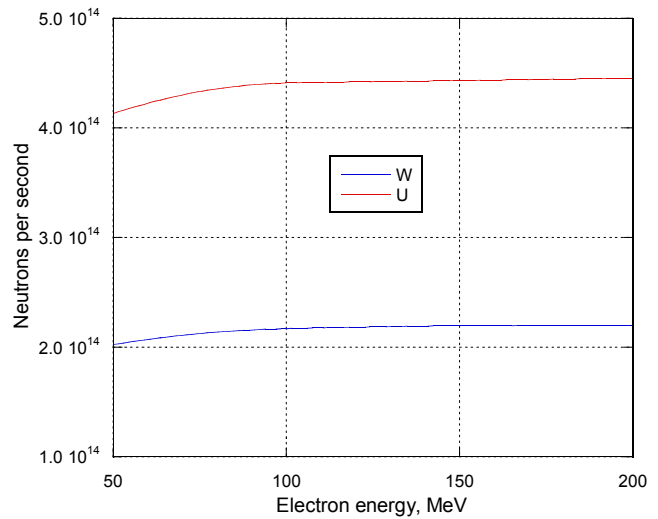


Figure 5. Neutron Source Strength from the Tungsten and the Uranium Targets as a Function of the Electron Energy with 100 kW Beam

The neutron spectrum from the target was analyzed as a function of the electron energy to quantify the high energy component. No significant differences were observed from using different electron energies as shown in Figure 6 for the uranium target material. Similar to the fission spectrum, the peak value of the neutron spectrum is less than 1 MeV. The magnitude of the high energy component of the spectrum is very small as shown in Figure 6. The neutron spectra from tungsten and uranium are similar allowing the use of either material in the subcritical assembly. The higher neutron yield from the uranium target increases the neutron flux in the subcritical assembly.

The target length should be adequate for stopping the electrons. However, the extra target material interacts with the generated neutrons that leave the target in the electron beam direction. A study was performed to define the required target length. Figure 7 shows the neutron yield as a function of the uranium target length. In the first several centimeters of the target length, most of the neutrons are generated from the electrons and (n, xn) neutron interactions. As the electron beam vanishes inside the uranium target material, the fission reactions caused by the forward neutrons slightly increase the neutron yield. At the target length of about 0.08-m, the neutron yield increase becomes negligible. Therefore, a 0.08-m uranium target length is selected. For tungsten material, the number of neutrons per electron increases as the target length increases to reach a maximum value at about 0.069 m. The extra tungsten target length acts as a neutron absorber, and slowly reduces the neutron yield.

3.0 Thermal-Hydraulics Analyses

Heat transfer and thermal-hydraulics parametric studies have been performed to help defining the target mechanical configuration, the size of the water coolant channels, and the temperature distribution in the target materials. The 100-KW electron beam with $\sim 2\text{-KW/cm}^2$ uniform beam power density, the 7-m/s water coolant velocity inside the target manifold, and the 4-atm coolant pressure are used. Higher coolant velocity is also under consideration to enhance the target performance. The target material has a cylindrical geometry and its axis coincides with the beam tube axis. The flow direction of the water coolant is perpendicular to the target axis. This arrangement results in a stack of disks forming the target design. The water coolant channels between the target disks have a constant thickness of 1.75 mm. The average increase in the water coolant temperature is less than 5 °C for the current coolant conditions. Each target disk is cooled from both sides to minimize its thermal deformation. The water coolant channels are connected in parallel to the input and the output manifolds. The analyses defined the thickness of the different target disks for limiting the maximum surface temperature to about 80 °C, for the electron energy in the range of 100 to 200 MeV. This surface temperature was selected to provide about 65 °C margin away from the water boiling temperature. Both target materials are placed inside an aluminum alloy cylinder. The thickness of the cylinder is 2 mm and the thickness of the beam window is also 2 mm. The uranium disks have a 0.7-mm aluminum clad to avoid water coolant contamination with fission products.

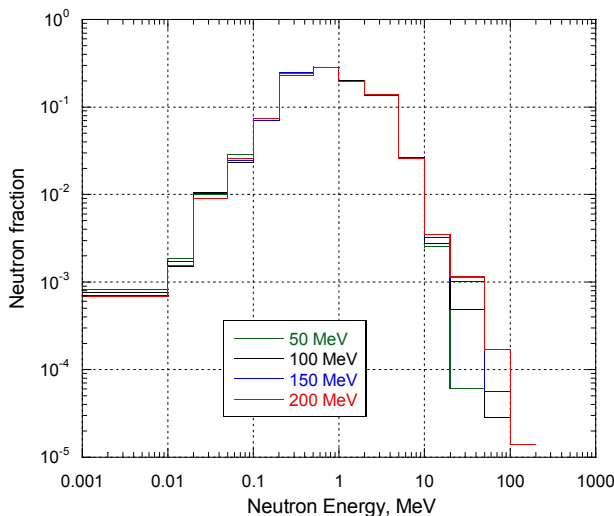


Figure 6. Normalized Neutron Spectra from Uranium Target as a Function of the Electron Energy

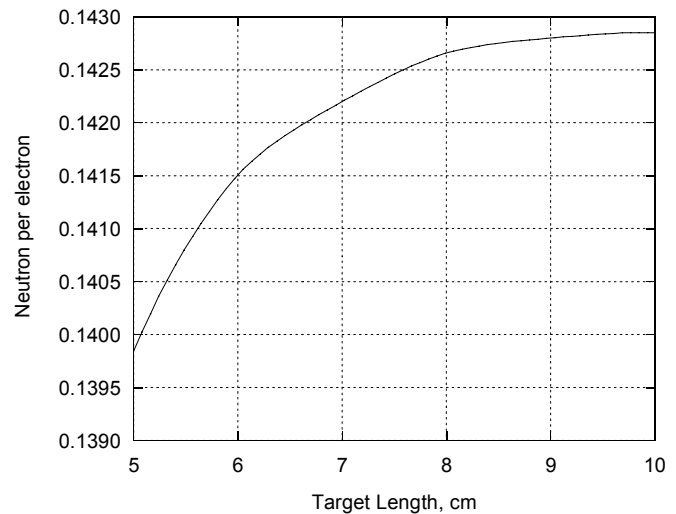


Figure 7. Neutron Yield per Electron as a Function of the Uranium Target Length

The results from the MCNPX studies using three-dimensional geometrical models were used for STAR-CD thermal hydraulics analyses. The three-dimensional geometrical models account for the target design details. The STAR-CD calculations were performed to define the thickness of each target disk according to the above design criteria. In these analyses, the water velocity field was calculated for each coolant channel and the spatial temperature profile was calculated for each target disk and each coolant channel using a single geometrical model for the target assembly and the three-dimensional MCNPX energy deposition results. Figure 8 shows the energy deposition profile in the uranium material from the MCNPX calculation. The flow field turbulence is suppressed in the 1.75 mm wide channels between the target disks and dissipates quickly. The heat transfer from the heated disks is mainly limited to laminar flow. Furthermore, small recirculation zones appear near the

edges of the target disks, midway between the inlet and outlet channels resulting in hotspots that define the peak thermal stresses of the disks. Sample of the STR-CD results are shown in Figures 9 through 12. The three-dimensional temperature profile in the uranium material is shown in Figure 9 for the 100 KW uniform beam using 200 MeV electrons. In this case, the third target disk has the maximum power density and temperature. Figure 10 shows the front surface temperature and the midplane temperature of this disk. The maximum wall temperature is $\sim 70^{\circ}\text{C}$ less than the water coolant boiling temperature. The maximum water coolant temperature is $\sim 31^{\circ}\text{C}$ as shown in Figure 11. These temperatures satisfy the adopted temperature design criteria. The velocity field in the water channel between the second and the third target disks is shown in Figure 12 where small recirculation zones are visible. These recirculation zones are responsible for the local peak temperatures shown in Figure 10.

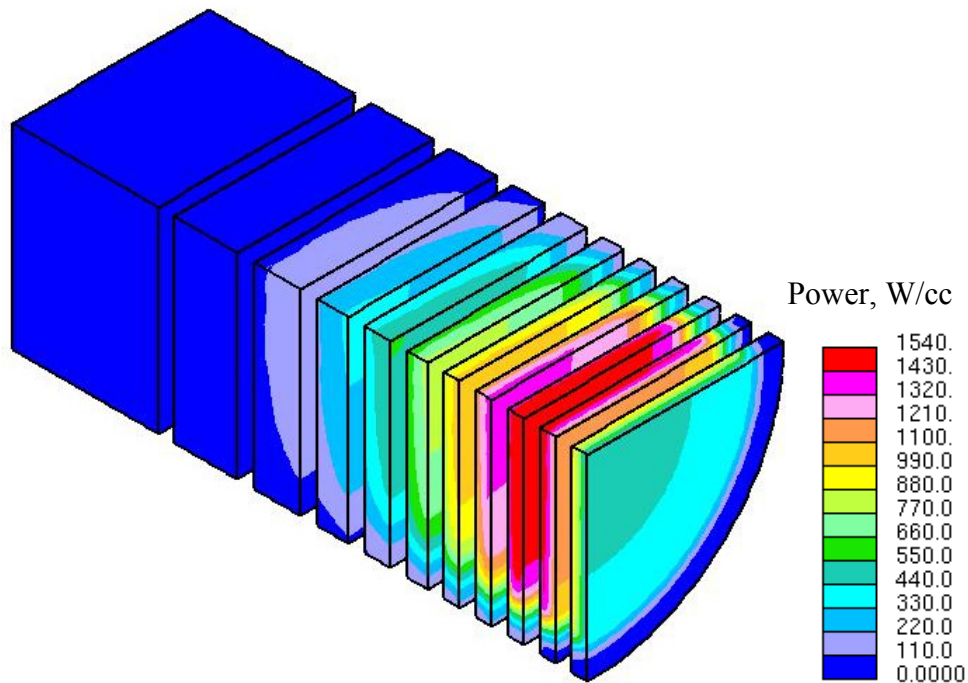


Figure 8 Energy Deposition Profiles of the Uranium Material Disks with 100 KW Uniform Beam Using 200 MeV Electrons

4.0 Thermal Stress Analyses

The three-dimensional model and the corresponding temperature profiles of the uranium and the tungsten targets were imported into NASTRAN computer code for thermal stress analyses. The intensity and distribution of the thermal stresses were evaluated for the normal operating conditions. In the target design, the disks are allowed to expand in the radial and axial directions to reduce the operating stresses. The thermal stress intensity distribution during the normal operation was evaluated. Although thermal stresses are secondary stresses, their maximum values are limited to a fraction of the material yield stress. This is a very conservative approach leaving a large design margin to account for radiation damage and thermal-cycling effects. These effects are under consideration to define the target operating lifetime.

For each target material, the analyses were performed for the 100 KW beam with electron energy of 100 and 200 MeV. The two electron energies were considered to insure a satisfactory target operation in the entire energy range. The energy deposition profiles and the spatial temperature distributions are quite different for these two electron energies. The tungsten target results show the peak thermal stress is less than 100 MPa.

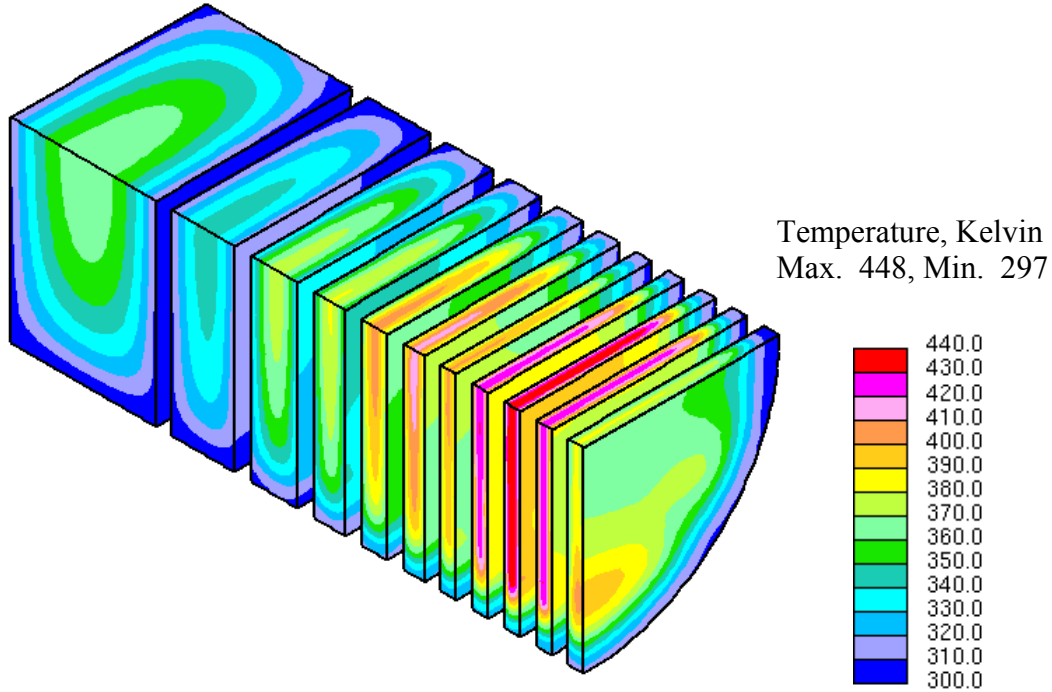


Figure 9 Temperature profiles of the Uranium Target Disks from the 100 KW Uniform Beam Using 200 MeV Electrons

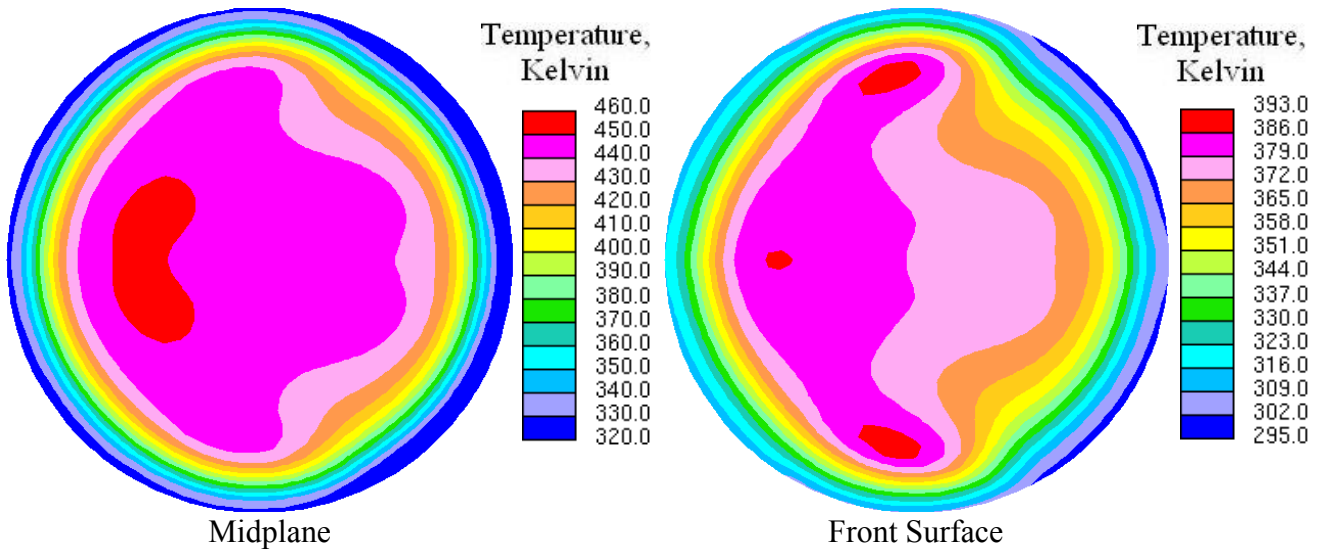


Figure 10 Midplane and Front Surface Temperature Distributions of the Third Uranium Disk from the 100 KW Uniform Beam Using 200 MeV Electrons

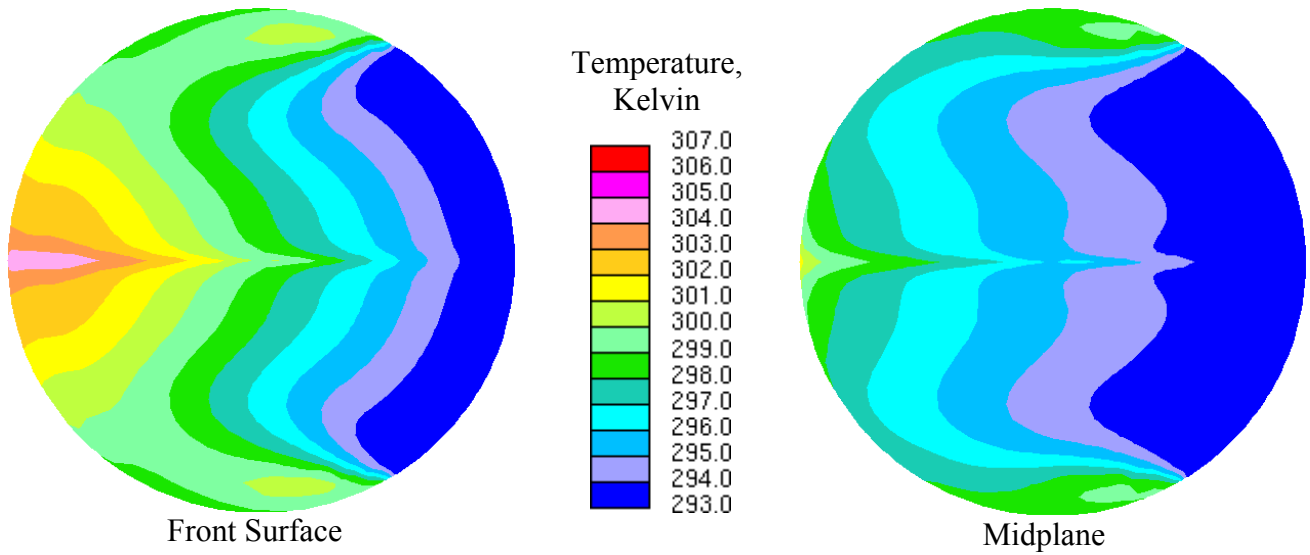


Figure 11 Front Surface and Midplane Temperature Distributions of the Coolant Channel between the Second and the Third Uranium Disks from the 100 KW Uniform Beam Using 200 MeV Electrons

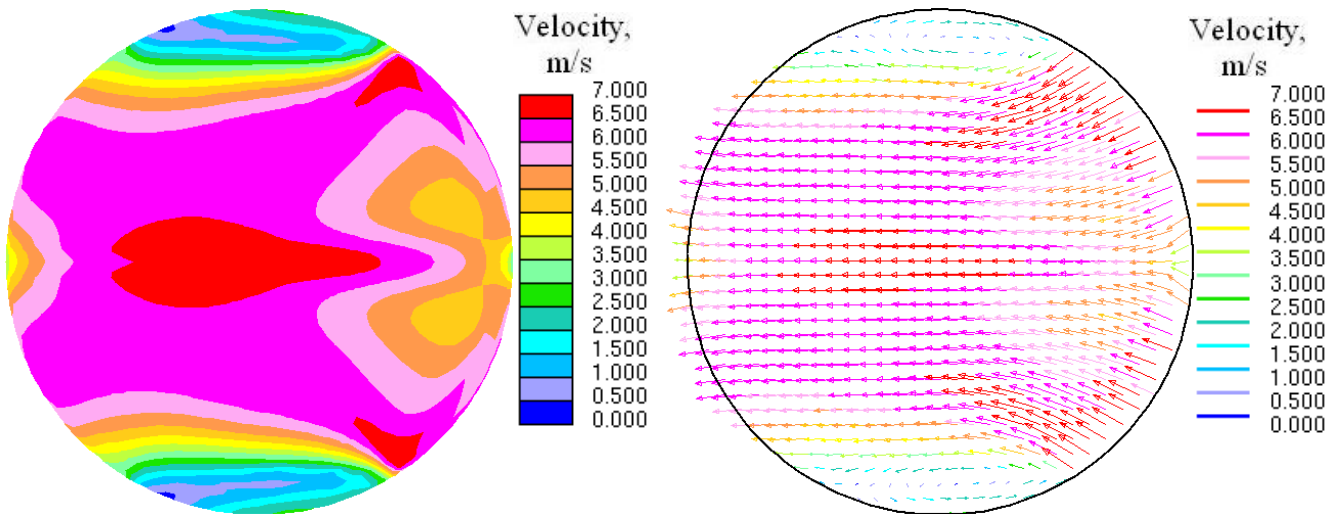


Figure 12 Midplane Flow Field of the Coolant Channel between the Second and the Third uranium Disks for the 100 KW Uniform Beam Using 200 MeV Electrons

5.0 Configurations and Performance Parameters of Tungsten and Uranium Targets

Physics, hydraulics, heat transfer, and thermal stress analyses have been iterated to define the target disk dimensions for tungsten and uranium materials. In the iteration process, the above design criteria are utilized. The resulting target disk thicknesses for both materials are given in Table 1. Uranium target requires thinner disks relative to tungsten because it has a higher energy deposition density and a lower thermal conductivity. The target mechanical design is the same for both materials except for the number and thickness of the target disks. Figure 13 shows an exploded view of the uranium target design for a subcritical assembly with hexagonal fuel elements.

The neutron yield and the neutron spectrum were calculated for the target designs using detailed three-dimensional models that include the coolant, the structure material, and the geometrical details of the mechanical design. The calculated neutron yield for the tungsten target is 0.0584 neutrons per electron (n/e) generating 1.82×10^{14} neutrons per second (n/s) from the 100 KW beam. For the uranium target, the neutron yield is 0.1067 n/e and the corresponding neutron intensity is 3.331×10^{14} n/s. The effect of the aluminum structure and the water coolant on the neutron yield was analyzed by repeating the analyses without including these materials. The effect amounts to a fraction of a percent increase, which is negligible. In addition, the results show that the obtained neutron spectra are very similar to the neutron spectra obtained from pure target materials.

Table 1. Tungsten and uranium targets disk thicknesses

Target Material	Disk Thickness, mm										
Tungsten	3	3	3	3	4	7	13	33	—	—	—
Uranium	3	3	3	3	3	4	5	6	9	12	28

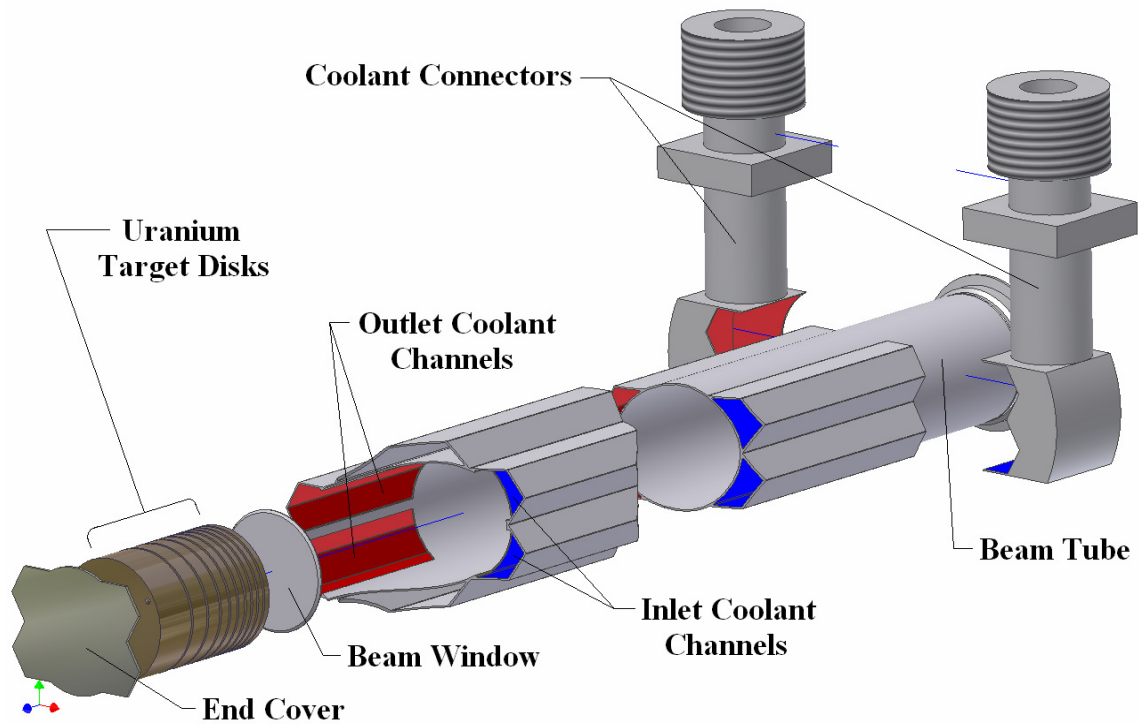


Figure 13. Exploded View of the Uranium Target Design for Hexagonal Fuel Elements

The spatial neutron source distribution is analyzed to maximize the neutron utilization in the sub-critical assembly. The neutron fraction that leaves the target along the beam axis has the potential of leaking out without utilization. The neutrons leaving from the electron beam window (top fraction) exits the system through the vacuum beam tube or interacts with the beam tube structure. A fraction of these neutrons reaches the sub-critical assembly by leaking from the beam tube. Also, the neutrons leaving the target in the beam direction (bottom fraction) interact with the water coolant and the reflector material under the target, which reduce their chances for reaching the sub-critical assembly. Table 2 shows the neutron source fractions leaving the tungsten and uranium target outer surfaces. Three cases are given for each target design. The first case has only the target disks and

the water coolant without the six channels around the target disks. The neutron source was tallied around the three surfaces of a cylinder containing the target disks. The other two cases include the six channels around the target as shown in Figure 13. Four channels are used for the coolant manifolds and the other two channels have water cooled beryllium. In the second case the neutron source was tallied around the external surfaces of the six channels, the top surface of the beam window, and the bottom surface of the target assembly. This model was extended to the full length of the sub-critical assembly for the third case. The neutron source was tallied to compare the neutron source fraction for the three cases.

The results show that a large neutron fraction leaves the target through the side surface. The fraction of neutrons that leave through the bottom section of the target is small. These neutrons will interact with the water coolant and the reflector material under the target and a fraction of these neutrons reach the sub-critical assembly, depending on the target's location along the sub-critical assembly axis. The neutron fraction leaving the target through the beam entry surface is around 0.25 of the total neutrons produced. However, most of these neutrons leak through the target beam tube to the sub-critical assembly as demonstrated by the results of the third case. Since the bottom neutron fraction is very small relative to the top fraction, this will impact the axial location of the target assembly inside the sub-critical multiplier for the optimum utilization. The third case results show that the neutron utilization will be more than 98.9% and it is quite satisfactory. The axial neutron source distribution was analyzed for both target materials. In both cases, the fourth disk has the peak value of the distribution for the 200 MeV electrons and this peak value location is shifted from the peak value of the nuclear heat deposition.

Table 2. Neutron Source Fraction from Tungsten and Uranium Targets

Surface	Target Disks	Target Assembly (Target Length)	Target Assembly (Core Length)
Tungsten Target			
Side	0.7224	0.6390	0.9886
Bottom	0.0422	0.0639	0.0008
Top	0.2354	0.2970	0.0106
Uranium Target			
Side	0.7635	0.6991	0.9906
Bottom	0.0247	0.0374	0.0010
Top	0.2118	0.2635	0.0085

6.0 Conclusions

In this conceptual design activity, Argonne National Laboratory has developed conceptual target designs for generating neutrons to drive the planned subcritical assembly at Kharkov Institute of Physics and Technology of Ukraine. The target design analyses defined the electron beam parameters and the targets performance. Tungsten and uranium are the most appropriate target materials for this application. For fixed beam power, electron energy greater than 100 MeV provides the maximum possible neutron source strength. The target design has a low pressure water coolant,

which facilitates the target design and the integration with the water-pool of the subcritical assembly. A beam power density of $\sim 2 \text{ KW/cm}^2$ is selected, it is based on the target analyses for satisfying the engineering requirements and minimizing the target cross section area. The calculated neutron yield from the tungsten target is 0.0584 neutrons per electron (n/e) and the corresponding neutron intensity is 1.82×10^{14} neutrons per second (n/s) for the 100-KW uniform beam with 200-MeV electrons. For the uranium target, the neutron yield is 0.1067 n/e and the neutron intensity is 3.33×10^{14} n/s for the same beam parameters.

Acknowledgments

Argonne National Laboratory's work was supported by the U.S. Department of Energy, Office of Global Nuclear Material Threat Reduction (NA212), National Nuclear Security Administration, under contract W-31-109-Eng-38.

References

1. Yousry Gohar, Igor Bolshinsky, Dmitry Naberezhnev, Jose Duo, Henry Belch and James Bailey, "Accelerator-driven subcritical facility: Conceptual design development," *Nuclear Instruments and Methods in Physics Research Section A*, *In Press*.
2. Y. Gohar, J. Bailey, H. Belch, D. Naberezhnev, P. Strons, and I. Bolshinsky, "Accelerator-Driven Sub-critical Assembly: Concept Development And Analyses," Proceeding of The RERTR-2004 International Meeting on Reduced Enrichment for Research and Test Reactors, Vienna, Austria, November 7-12, 2004.
3. J. Hendricks, G. McKinney, L. Waters, et al., "MCNPX, Version 2.5.E," Los Alamos Report, LA-UR-04-0569, February 2004.
4. STAR-CD Version 3.1B, CD-Adapco Group.
5. MSC. Nastran Software, MSC. Software Corp., Inc.